International Journal of Air-Conditioning and Refrigeration Vol. 15, No. 4 (2007) 175~181

Modelling of a High Efficiency Refrigeration System with Heat Storage for Reverse Cycle Hot Gas Defrost

Ardiyansyah[1], Kwang-Il Choi[1], Jong-Taek Oh[2,*], Hoo-Kyu Oh[3]

[1]*Graduate School, Chonnam National University, Yeosu, Chonnam 550-749, Korea*
[2]*Dept. of Refrigeration and Air Conditioning Eng., Chonnam National University, Yeosu, Chonnam 550-749, Korea*
[3]*Dept. of Refrigeration and Air Conditioning Eng., Pukyong National University, Busan 608-739, Korea*

(Received September 6, 2007; revision received December 17, 2007)

Abstract

A computer model of a high efficiency refrigeration system equipped with heat storage for reverse cycle-hot gas defrost (the stored heat is used during defrost cycle of the system) is presented. The model was developed based on both theoretical and empirical equations for the compressor, evaporator, condenser and the heat storage equipment. Simulations of the prototype system were carried out to investigate refrigeration system performance under various operating conditions during refrigeration cycles. The simulations of the evaporator during defrost cycles at 30 and 40℃ hot gas refrigerant temperature were also performed which resulted on shorter defrost time but only slight increase in defrost efficiency. These information on energy efficiency and the defrost time required are important in order to avoid excessive parasitic load and temperature rise of the refrigerated room.

Key words: Heat Storage; Refrigeration system; Performance; Simulation; Reverse cycle; Hot gas Defrost

Nomenclature

A : area [m^2]
C_p : specific heat [J/kgK]
h : enthalpy [J/kg]
$\dot{m}$: mass flow rate [kg/s]
M : mass of water [kg]
P : compressor power [W]
q : heat transfer rate [W]
Q : heat energy [J]
t : operation time [s]
T : temperature [K]
U : overall heat transfer coef. [kW/m^2K]

Greek symbols

ε : heat exchanger efficiency

Subscript

1-4 : state points
a, in : evaporator air inlet
a, out : evaporator air outlet
b, in : condenser air inlet
b, out : condenser air outlet
c : condenser
cw : evaporator coil wall
e : evaporator
f : frost
g : gas
l : liquid
r : refrigerant
s : stored energy
sp : single-phase
tp : two-phase
th : heat storage
v : vaporization
w : water

*Corresponding author. Tel.: +82-61-659-3273, Fax: +82-61-659-3279
E-mail address: ohjt@chonnam.ac.kr

1. Introduction

Reciprocating refrigeration systems have been used in wide ranges of commercial application, including transportation refrigeration systems. Many studies have been carried out in order to increase the energy

efficiency of the system. One of the considerations is the accumulation of frost in the evaporator during its operation below the freezing point of water and high humidity environment. Frost formation increases the thermal resistance between the fin and the air flow, hence decreasing the heat transfer processes in the evaporator. Frost also blocks air flow, increasing the pressure drop of the refrigerated air. Both effects reduce the refrigeration capacity and the performance of the system. To overcome these problems, the defrosting process should be performed periodically. One of the methods is the reverse cycle-hot gas defrost which is used widely in industrial refrigeration applications[1].

In the present study, a refrigeration system equipped with heat storage for a reverse cycle-hot gas defrost is modeled. During the refrigeration cycle, the equipment acts as a pre-condenser and stores a portion of refrigerant heat rejection as depicted in Fig. 1. During the defrost cycle, the system uses heat from refrigerant gas discharged from the compressor, to defrost the evaporator coils.

Various computer or numerical models have been developed based on physical theories, empirical correlations using the curve fitting method, or combination of both. This model uses physical equations combined with the curve fitting empirical correlations to develop a model with simple and minimum input requirements. Based on the system operating conditions, refrigeration system models can be divided into steady-state[2-4] and transient models[4-6]. The steady-state model was used in this study with the following reasons: in the transportation refrigeration systems, the equipment was mainly intended to keep the refrigerated room in steady-state conditions within the set temperature range. Also, the cargo being carried was already under low temperature conditions when it was loaded[3].

The objective of this study is to develop a computer model which can be used to analyze the effects of various operating variables on the performance of refrigeration system equipped with heat storage during the steady-state refrigeration cycles. Further simulation of the evaporator coils defrosting process is also studied to obtain quantitative information on energy efficiency and the defrost time required which is important to avoid excessive parasitic load and temperature rise.

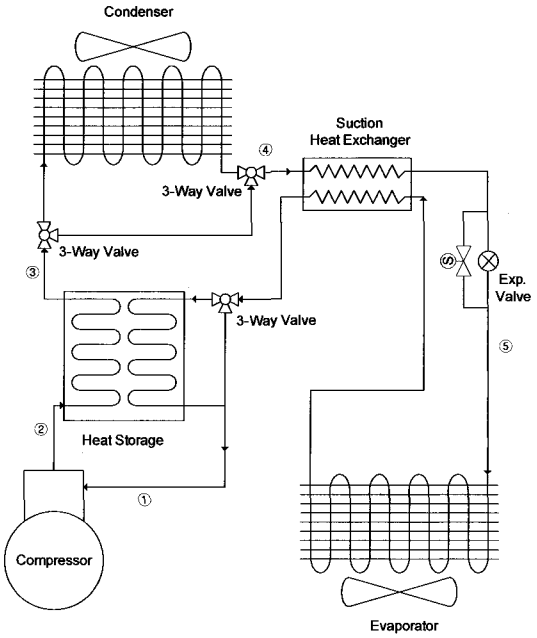

Fig. 1. Schematic of refrigeration system equipped with heat storage.

2. Refrigeration system analysis

2.1 Model Development

The heat storage equipment uses water or brine which stores the heat. During the defrost process, the system directs hot refrigerant from compressor through the heat storage (bypassing the condenser) to the evaporator for defrosting the evaporator coils. The refrigerant ejects its heat and condenses into liquid. It then flows back into the heat storage equipment. The refrigerant is re-evaporated by the heat stored in the equipment before entering the compressor and circulates again.

A steady state energy balance equation over the entire system is described in equation (1)

$$P + q_e = q_c + q_{th} \tag{1}$$

The simplified p-h diagram of the system is depicted in Fig. 2. The reciprocating, semi-hermetic type, compressor was modeled based on published manufacturers' rating data based on curve fitting method. The corresponding equations take the following form:

$$X = f(T_e,\ T_c) \tag{2}$$

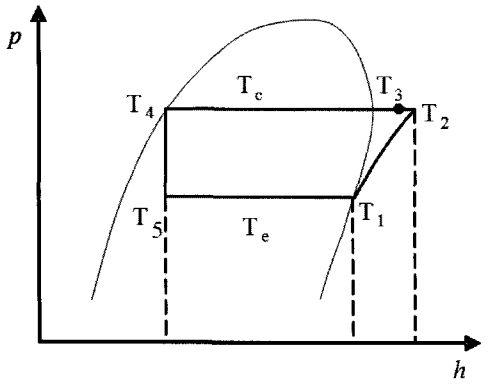

Fig. 2. Simplified p-h diagram of refrigeration cycle.

where X is the refrigeration capacity, compressor power consumption or the refrigerant mass flow rate.

The direct-expansion evaporator was modeled based on the single zone heat transfer process. The two-phase refrigerant heat transfer process between the refrigerant inside the evaporator coils and the air flow were derived from the ε -NTU relation for two-phase heat exchanger[7] as described in equation (3).

$$UA_e = \left(\frac{1}{h_a\left(A_{tube} + \eta_{fin}.A_{fin}\right)} + \frac{t_{tube}}{k.A_{wall}} + \frac{1}{h_r.A_r} \right) \quad (3)$$

where k and t_{tube} is the tube heat conductivity and thickness respectively.

A quasi-steady state approach was applied to the heat transfer process in the heat storage area. For a determined period of time, the heat storage temperature increased[8] by eq. (4):

$$\Delta T_w = (T_2 - T_w)\frac{\dot{m}.c_p}{M.c_v}\left[1 - \exp\left(-\frac{UA_{th}}{\dot{m}.c_p}\right)\right].\Delta t \quad (4)$$

The overall heat transfer coefficient for heat storage was estimated as such it could store sufficient heat during 4 hours refrigeration cycles.

The air-cooled condenser used in this study was modeled based on two-zone analysis, namely supercooling and condensation zones. The refrigerant leaving the condenser was assumed to be in a saturated liquid phase. The heat transfer within the supercooling was obtained from equation (5) and (6) where ε_c is condenser heat transfer effectiveness. The two-phase heat transfer for the condensation zone is given in (7).

$$q_{c,sp} = \dot{m}_r c_r (T_3 - T_{b,in})\varepsilon_c \quad (5)$$

$$\varepsilon_c = 1 - \exp\left[-\frac{\dot{m}_a c_a}{\dot{m}_r c_r}\left(1 - \exp\left(\frac{U_{c,sp} A_{c,sp}}{\dot{m}_a c_a}\right)\right)\right] \quad (6)$$

$$q_{c,tp} = \dot{m}_b c_a (T_c - T_{b2})\left[1 - \exp\left(\frac{U_{c,tp} A_{c,tp}}{\dot{m}_b c_b}\right)\right] \quad (7)$$

The corresponding overall heat transfer coefficient for each zone was obtained from heat exchanger equation similar to equation (3) for the condenser.

R-22 properties used in the analysis were obtained from data generated by REFPROP 6.0 software. The air side heat transfer coefficients for both evaporator and condenser were calculated using the correlation from Wang[9]. The Gungor-Winterton correlation[10] was used for the two-phase heat transfer coefficient.

2.2 Simulation algorithm

The flowchart of the computer algorithm is described in Fig. 3. The refrigeration system analysis was reduced into the solution of simultaneous equations at the balance point of the system and solved using Newton-Raphson approach. At each determined time step, the program solved the equations and generated operating variable values for the corresponding condition. Then, the increase in the heat storage temperature as given by equation (4) was used to update the water temperature inside the heat storage area. The water temperature affected the operating parameters at the balance point; therefore, the program was repeated again to find the new balance point. The program ran until the determined operation time was reached.

The program results include evaporating and condensing temperatures, refrigeration capacity, compressor power consumption, refrigerant mass flow rate, condenser heat ejection, system coefficient of performance, heat storage temperature and heat the energy available in the heat storage equipment.

3. Evaporator coils defrosting analysis

During the defrost process, the evaporator fan is shut-down hence the heat and mass transfer process between frost and air inside the refrigerated room is in a natural convection mode. In this study, the following simplifications are considered: the refrigerant

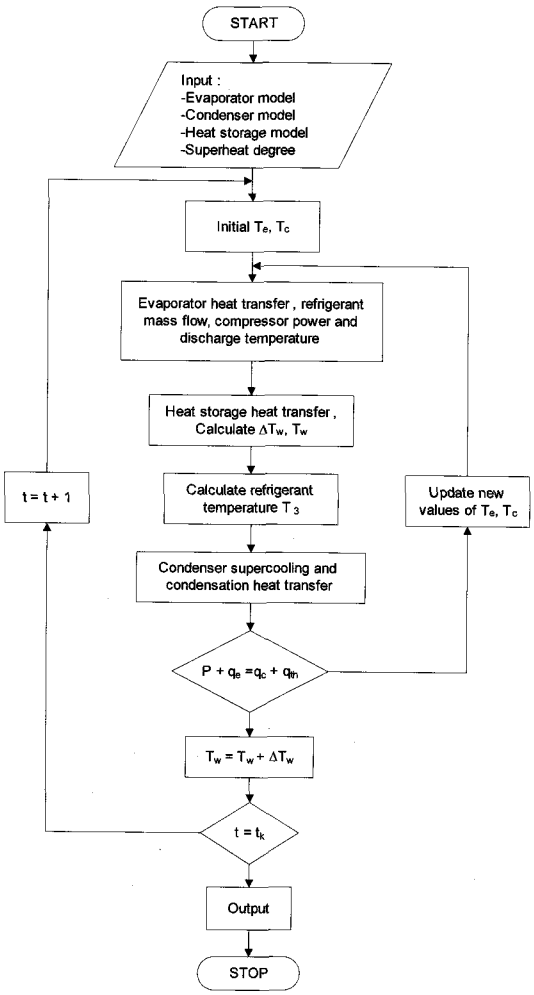

Fig. 3. Flowchart of the computer algorithm.

phases are in thermodynamic equilibrium, the frost mass per heat exchanger unit area and defrosting rate are uniform in all evaporator sections, and the heat conduction in the axial direction of the pipe is negligible.

During the defrost process, part of the heat is stored in the coil, frosts and surface water and the remainder is transferred from the refrigerant to the coil, frost, surface water and the ambient air. Krakow[11] divided the process into preheating, melting, vaporizing and dry heating stages. The energy equation for each heat exchanger element is described as:

$$Q_r = Q_s + Q_c + Q_f + Q_v \tag{8}$$

Each energy components are described in equations (9)-(12). Q_s is the stored heat energy in tube and fin, frost or surface water, which depends on the corresponding stages during the process. Q_c is the convective heat released into the ambient air and is a function of air film conductance h_a, surface area and temperature of the surface and ambient air. Q_f is the heat energy conducted from the coils to the frost, where h_{aw} and T_f are air/water film conductance and frost temperature respectively. The heat from condensing refrigerant is also used to vaporize surface water that resulted from melted frost, described as Q_v and depends on the rate of mass vaporization (R_v) and the enthalpy of vaporization of water (h_{fg}).

$$Q_s = C\frac{dT}{dt} \tag{9}$$

$$Q_c = h_a A_{eff}(T_{cw} - T_a) \tag{10}$$

$$Q_f = h_{cw} A_{eff}(T_{cw} - T_f) \tag{11}$$

$$Q_v = R_v h_{fg} \tag{12}$$

The rate of vaporization was assumed to be proportional to the difference between water vapor density at the wall temperature and water vapor density at ambient temperature, effective wetted area of the coil and surface water vaporization coefficient, as described in Krakow[11]. The value of air film conductance, air/water film conductance and rate of vaporization obtained experimentally by Krakow[11] were used in this study.

The simulation was conducted by dividing the process into small time steps and applying the energy equations for each time step. The preheating stage was analyzed from the beginning of the defrost process and terminated when the coil wall temperature T_{cw} approached 0℃. The melting stage ended and the vaporizing stage began when the frost mass, m_f reached 0. The dry heating stage was not considered, the defrost process ended when the surface water that resulted from the melted frost was completely vaporized.

4. Results and dscussion

4.1 Refrigeration cycles simulation

The model was used in simulations of various operating conditions. Seven different return air tempera-

tures of the refrigerated room were used to analyze the effects on system performance. The evaporator fan air flow rates of 1,000, 1,500 and 2,000m^3/h were also used as input for the model.

Fig. 4 and 5 show the effect of the refrigerated room temperature and the air flow rate on the refrigeration capacity and the compressor power consumption, respectively. As expected from the performance trends of actual refrigeration systems, when the refrigerated room return air temperature was increased, the refrigeration capacity increased as depicted in Figure 4, the refrigeration capacity also increased significantly.

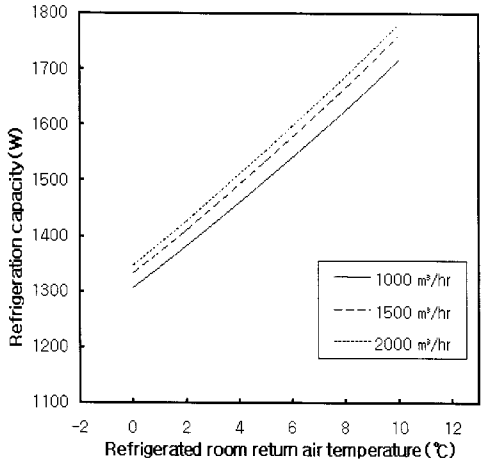

Fig. 4. The effect of refrigerated room temperature and evaporator air flow rate on capacity.

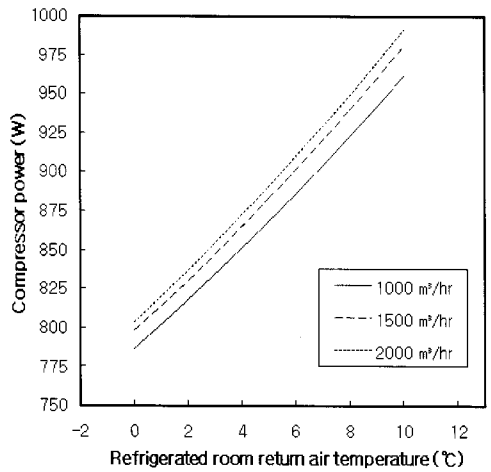

Fig. 5. The effect of refrigerated room temperature and evaporator air flow rate on compressor power.

At higher refrigerated room temperature, more compressor power was required to achieve suitable performance at the balance point of the system; hence as can be inferred from Figure 5, compressor power increased as the refrigerated room returns air temperature raised. In Figure 6, the system COP slightly increased as the return air temperature increased. This was mainly caused by the significant increase in refrigeration capacity. The heat storage temperature increase during finite time steps for three different masses of water is depicted in Figure 7. It can be inferred that the finite difference heat transfer processes in the heat storage equipment became negligible when the temperature of the water approached the temperature of the refrigerant gas discharged from the compressor.

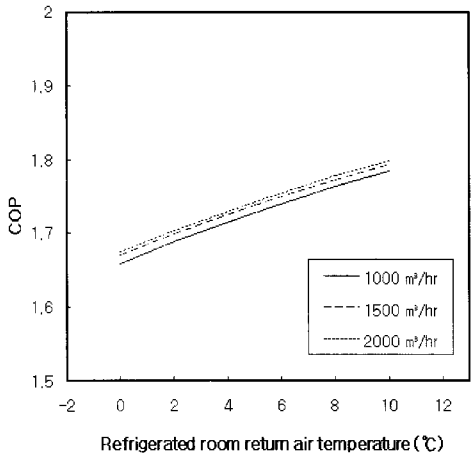

Fig. 6. The effect of refrigerated room temperature on COP.

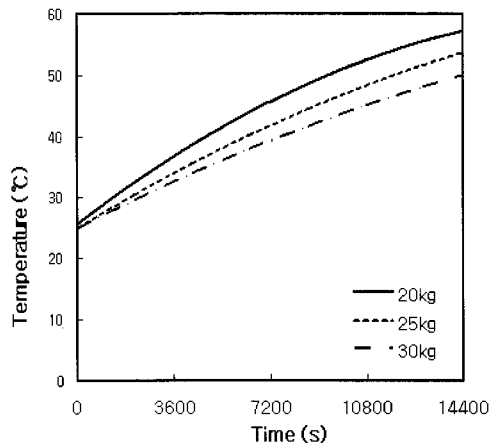

Fig. 7. Heat storage temperature over time step for three different water mass.

Table 1. Defrost process energy distribution.

Hot gas refrigerant temperature(℃)	Defrost time (s)	Energy stored, Q_s (%)	Energy to vaporize surface water, Q_v (%)	Energy convected, Q_c (%)	Defrost deficiency Q_f (%)
30	412	31.7	27.3	18.4	22.6
40	378	26.2	27.6	23.2	23

4.2 Evaporator coils defrost simulation

The heat transferred from the hot refrigerant during the defrost process was not only used to melt the frost, part of the energy was stored in the coils, frost, and surface water, and was absorbed during the vaporization of the surface water and convected to the ambient air. This unavoided excess energy became part of cooling load during the next refrigeration cycle. The simulation results for refrigerant gas temperatures of 30 and 40℃ were used to analyze the energy distribution during the defrost process and are listed in Table 1.

The defrost efficiency, as used by Cole[12], was defined as the ratio of the energy used to melt the frost and the total energy provided during the defrost process. As depicted in Table 1, using a higher hot gas refrigerant temperature decreased the defrost time. However, only a small improvement of defrost efficiency was obtained from the simulation and the higher convective heat that resulted may lead to excessive increases in refrigerated room air temperature during the defrost process.

5. Concluding remarks

A computer model for refrigeration systems equipped with heat storage for the reverse cycle hot gas defrosts method was developed based on physical equations and empirical correlations. The model can be used to simulate the influence of various operating variables on the performance of refrigeration systems during steady-state refrigeration cycles. Predicted refrigeration capacity, compressor power and COP were increased with higher refrigerated room temperature setting and evaporator air mass flow. Further study on the simulation of the evaporator coil during defrost process with hot gas refrigerant temperatures were also conducted to obtain quantitative information on the defrost time required and defrost energy efficiency. Simulation on higher hot gas refrigerant temperature resulted shorter defrost time but only slight increase in defrost efficiency.

Acknowledgements

The authors wish to acknowledge that this work was supported by the Ministry of Maritime Affairs and Fisheries of Korea (KIMST Grant No. 20060090) and Jeil SPV Co.

References

[1] Hoffenbecker, N., Klein, S.A., Reindl, D.T., 2005, Hot Gas Defrost Model Development and Validation, Int. J. Refrig. 28: 605-615.

[2] D.J. Swider, M.W. Browne, P.K. Bansal, V. Kecman, 2001. "Modeling of Vapor- Compression Liquid Chillers with Neural Networks", App. Thermal Eng. 21: 311-329.

[3] Jolly, P.G., Tso, C.P., Wong, Y.W. and Ng, A.M., 2000, Simulation and Measurement on the Full Load Performance of Refrigeration System in a Shipping Container, Int. J. Refrig. 23: 112-126.

[4] Koury, R.N.N., L. Machado and K.A.R. Ismail, 2001, "Numerical Simulation of A Variable Speed Refrigeration System", Int. J. Refrig. 24: 192-200.

[5] O'Neal, D.L., Peterson K.T., Anand N.K., Schliesing J.S., 1989. "Refrigeration System Dynamics During the reverse Cycle Defrost", ASHRAE Trans. 95: 689-698.

[6] Browne, M.W., P.K. Bansal, 2002. "Transient Simulation of Vapor-Compression Package Liquid Chillers" Int. J. Refrig. 25: 597-610.

[7] Incropera, Frank. P. and David P. DeWitt 1990, Fundamental of Heat and Mass Transfer 3rd ed., Wiley and Son, Singapore.

[8] Boeis A.M., K.O. Homan, J.H. Davidson, Wei Liu, 2005. "A Variable Effectiveness Model for Indirect Thermal Storage Devices" Proc. of ASME Summer Heat Trans. Conference" HT2005-72711 Research 25: 859-880.

[9] Wang, Chi-Chuan, Kuan-Yu Chi, Chun-Jung Chang, 2000, Heat Transfer and Friction Characteristics of Plain Fin-and-tube Heat Exchangers, part II: Correlation, Int. J. of Heat and Mass Trans. 43: 2693-2700.

[10] Gungor, K.E., & Winterton, R.H.S., 1987, Simplified General Correlation for Saturated Flow Boiling and Comparisons of Correlations with Data, Chem. Eng. Research and Design 65: 148-156.

[11] Krakow, K.I., S.Lin, L. Yan, 1992, A Model of Hot-Gas Defrosting of Evaporators, ASHRAE Trans. 98(1): 451-474.

[12] Cole, R.A., 1989, Refrigeration Loads in a Freezer Due to Hot Gas Defrost and Their Associated Costs, ASHRAE Trans. 95(2): 1149-1154.